This paper was recommended for publication in revised form by Regional Editor Ahmed Kadhim Hussein

NUMERICAL SIMULATION ON THE EFFECT OF LATENT HEAT THERMAL ENERGY STORAGE UNIT

Abdel Illah Nabil KORTI
ETAP laboratory, University of Tlemcen, FT, Department of Mechanics,
BP 230, 13000 Tlemcen, Algeria

ABSTRACT

Thermal energy storage is a practical and important way in conserving available energy and improving its utilization. Unlike the sensible heat storage method, the latent heat storage method provides much higher storage density, with a smaller temperature difference between charging and discharging heat phase. This work presents a numerical study of a latent heat storage exchanger filled with phase change material (PCM). Water flows by forced convection through the inner tube and transfers the heat to PCMs. A mathematical model based on the conservation energy equations was numerically resolved by a commercial FLUENT 6.3.2 code. Several numerical investigations were conducted in order to examine the impact of the key parameters: mass quantity of PCM used, number of pass and the mass flow rate of the water. This parametric study provides guidelines for system thermal performance and design optimization.

INTRODUCTION

Solar radiation is intermittent by its nature. Its total available value is seasonal and dependent on the meteorological conditions of the location. Thermal Energy Storage (TES) is necessary for effective utilization of such energy source, to meet demand on cloudy days and at night. TES, therefore, plays an important role in conserving thermal energy, leading to an improvement in the performance and reliability of a range of energy systems. The heat storage occurs in the form of latent heat, sensible heat, or both. Compared with other heat storage methods, advantages of latent heat storage materials are that heat storage and delivery occur in a narrow temperature interval corresponding to their phase transition temperature and significantly smaller volume change before and after phase transition process.

Generally the phase change material have low thermal conductivity and expand on melting, therefore the design of a suitable heat exchanger is an important component of a latent heat storage system. Several investigators study different configurations of latent heat storage. An experimental investigation involving the effectiveness–NTU method was conducted by Amin [1] using PCM encapsulated in spheres. The study demonstrated that a correlation existed between the effectiveness of heat transfer and the mass flow rate in accordance with the effectiveness–NTU relationship. The correlation presented can be used to predict the average thermal capacity from the thermal energy storage (TES) system for a given flow rate. A numerical study was conducted by Basal [2] on a new type triple concentric-tube thermal energy storage system. The effects of different sizes of the tube radii on the performance of the proposed storage system are investigated and compared with conventional double-tube storage system. The results indicate that, a significant enhancement in the system performance can be achieved. The results show that the most important design parameters for a triple concentric-tube storage system are the radial location and the thickness of the PCM filled annulus. Karthikeyan [3] was performed a parametric studies on the performance of a packed bed storage unit filled with PCM encapsulated spherical containers, suitable for low temperature solar air heating applications. It is concluded that the three parameters of the balls sizes, temperature difference between the HTF inlet and the phase change temperature of the PCM, and the mass flow rate of the HTF, are influences the charging and decreasing process.

Some authors review the different types of PCMs and main criteria that govern their selection. Sharma [4] was summarized the investigation and analysis of the available thermal energy storage systems incorporating PCMs for use in different

applications. Rathod [5] was reported a detailed review for thermal stability of different groups of PCMs. The PCMs are categorized as organic (paraffins and non-paraffins), inorganic (salt hydrates and metallics) and eutectics (organic eutectics and inorganic eutectics). Further, a broad database of different PCMs is developed for which thermal cycling tests were carried out by different researchers and reported in the literature. Soares [6] provides a comprehensive review on previous studies related to the evaluation of how and where, PCMs are used in passive latent heat thermal energy storage systems, and how these construction solutions are related to building's energy efficiency. It was concluded that PCM can contribute to increase indoor thermal comfort, reduce energy consumption and contribute for the reduction of CO2 emissions associated to heating and cooling.

Selka et al. [7] was presented a 2D numerical study of using PCM a phase change material to improve thermal performance of building in Tlemcen city. A specific paraffin material was placed in brick wall to reduce the room temperature during a daytime. The numerical results show a significant temperature reduction inside the studied solar test room, about 6°C to 8°C and therefore, the energy consumption due to air conditioning is reduced which provides benefits to economic and environmental aspects. After, the same authors was presented a 2D model with a real size home composed of two-storey (ground and first floor spaces) separated by a slab, enveloped by a wall with rectangular section containing PCM [8]. The numerical results showed that the model can reduce the room temperature by about 6 to 7°C of temperature depending on the floor level (first floor spaces or ground floor spaces).

Castel [9] was presented an experimental study of a PCM tank for cold storage applications. It was also demonstrated that coil in tank designs are effective at delivering a constant outlet temperature and effective heat transfer with large surface areas. Darzi [10] was simulated plate type PCM storage numerically used in free cooling system. Results showed that increasing the Stefan number causes the increase of the cooling power and the outlet air temperature. Omojaro [11] was reported an experimental and modeling results on the transient performance of a latent thermal energy storage (PCM) heat exchanger under simultaneous charging and discharging operation. The simultaneous operation mode stores lesser energy based on the temperature difference but has 13% higher thermal efficiency for the operation set time. The study presented by Charzat [12] was to develop and validate a simulation model for the heat storage units comprising compact storage module panels filled with PCMs. The study showed that latent heat storage offers certain advantages over sensible heat storage and it attracts more attention even in the areas where it was not considered in the past.

The major objective of the present study is to investigate the effect of PCM on the performance of the latent heat thermal energy storage system for water heating applications. The effects of the PCM quantity, number of pass and fluid flow rate have been analyzed during charging and discharging processes.

SYSTEM DESCRIPTION AND MATHEMATICAL ANALYSIS

System description

TABLE 1. PHYSICAL PROPERTIES OF SP22A17 [13].

Parameters	values
Density ρ [kg/m^3]	1480
Heat capacity c_p [J/Kg K]	2500
Conductivity λ [W/mK]	0.6
Latent heat L_f [J/kg]	150,000
Solidus temperature [K]	295
Liquidus temperature [K]	297
Viscosity μ [kg/ms]	0.00011
Thermal expansion [K^{-1}]	0.001
Reference temperature de T_{ref}[K]	298

The physical model studied is a 2D exchanger filled with PCM (code SP22A17) from Rubitherm. This is a Hydrated Salt and Paraffin Wax Combination. A water tube passes through inside the PCM to store heat latent during sunny periods and recover it during deficit periods. The copper tube has a diameter of 14 mm and the thickness is assumed negligible. The geometric parameters of the model are shown in Fig.1. For the water tube, the radius of the outer arc is 48 mm and of the inner arc is 20 mm. The thermo-physical properties of SP22A17 are given in table (1).
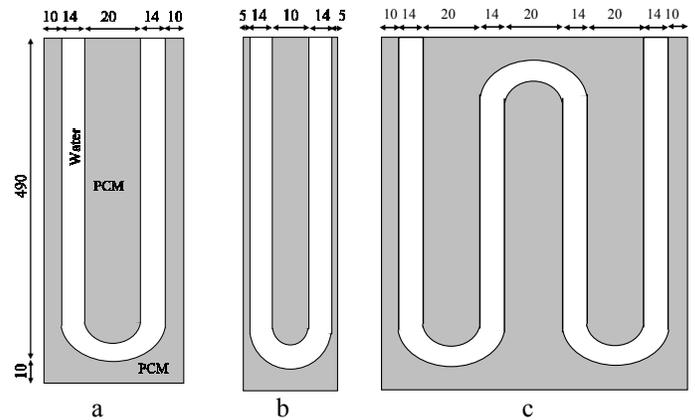
FIG. 1. GEOMETRIC CONFIGURATIONS OF THE STUDIED PROBLEM [mm].

Conservation of energy

The thermodynamic properties of PCM are supposed to be independent of temperature. The theory of mixtures is used to define the physical properties in a two-phase domain through a volumetric liquid fraction f_ℓ, where $0 \leq f_\ell \leq 1$. This gives (ℓ and s design the liquid and solid phases):

$$\rho = \rho_\ell f_\ell + (1 - f_\ell)\rho_s \tag{1}$$

$$\lambda = \lambda_\ell f_\ell + (1 - f_\ell)\lambda_s \tag{2}$$

600

$$c_p = c_{p\ell} f_\ell + (1 - f_\ell) c_{ps} \qquad (3)$$

To simulate the process of heat transfer with phase change, a single domain enthalpy method is used. The enthalpy of the material is defined as the sum of sensible heat $(h = c_p T)$ and latent heat ΔH, namely

$$H = h + \Delta H \qquad (4)$$

The latent heat ΔH in general can be expressed as

$$\Delta H = f_\ell L_s \qquad (5)$$

where L_s is the latent heat of solidification and f_ℓ is the local liquid fraction with value 1 representing liquid state and 0 for solid state. In general the local liquid fraction will depend on the nature of solidification. To simplify and focus subsequent discussions in the current work, the liquid fraction is taken to be a function of temperature alone. Different forms have been proposed for the relationship between the liquid fraction and the temperature. One of the simple forms is a linear relationship [14-15]:

$$f_\ell = \begin{cases} 1 & T > T_\ell \\ \dfrac{T - T_s}{T_\ell - T_s} & T_s \le T \le T_\ell \\ 0 & T < T_s \end{cases} \qquad (6)$$

where T_ℓ and T_s are, respectively, the liquidus and solidus temperature.

The conservation of thermal energy in the process can be expressed in terms of temperature in the form [14-15]:

$$\rho C_p \left(\frac{\partial T}{\partial t} + u \frac{\partial T}{\partial x} + v \frac{\partial T}{\partial y} \right) = \lambda \left(\frac{\partial T^2}{\partial x^2} + \frac{\partial T^2}{\partial y^2} \right) + S_T \qquad (7)$$

The source term S_T which embodies the latent heat of fusion can be derived to be

$$S_T = -\rho L_S \left(\frac{\partial f_\ell}{\partial t} + u \frac{\partial f_\ell}{\partial x} + v \frac{\partial f_\ell}{\partial y} \right) \qquad (8)$$

Momentum equation

The momentum equation of the fluid flows is governed by the unsteady Navier-Stokes equations in the Boussinesq approximation. In order to consider the phase change, we utilize Darcy's source term for handling the fluid flow in the solidifying molten metal pool. With the assumption of the constant density, the momentum equation in the liquid saturated porous medium can be expressed as the following form

$$\rho \left(\frac{\partial u}{\partial t} + u \frac{\partial u}{\partial x} + v \frac{\partial u}{\partial y} \right) = -\frac{\partial p}{\partial x} + \mu \left(\frac{\partial^2 u}{\partial x^2} + \frac{\partial^2 u}{\partial y^2} \right) + S_u \qquad (9)$$

$$\rho \left(\frac{\partial v}{\partial t} + u \frac{\partial v}{\partial x} + v \frac{\partial v}{\partial y} \right) = -\frac{\partial p}{\partial y}$$
$$+ \mu \left(\frac{\partial^2 v}{\partial^2 x} + \frac{\partial^2 v}{\partial y^2} \right) + \rho g \beta (T - T_{ref}) + S_v \qquad (10)$$

Where u the x-velocity component, v the y-velocity component, P the pressure, T the temperature, T_{ref} the reference temperature, H the enthalpy, μ the dynamic viscosity, g the gravitational acceleration, β the thermal expansion coefficient. Darcy source term (S_u and S_v) automatically ensures that the velocity in the fully solidified control volumes vanishes [14-15].

$$S_u = -A \frac{(1 - f_\ell)^2}{(f_\ell^3 + \varepsilon)} u \text{ and } S_v = -A \frac{(1 - f_\ell)^2}{(f_\ell^3 + \varepsilon)} v$$

A is the porosity and ε is a small positive number introduced to avoid division by zero.

Continuity equation is given by

$$\frac{\partial u}{\partial x} + \frac{\partial v}{\partial y} = 0 \qquad (11)$$

Initial and boundary conditions:

At the entrance of the channel a fixed mass flow (0.01 kg/s.) and temperature (313 K charged period and 293 K during discharged period) are imposed.

At the exit, a fully developed flow is assumed by imposing a zero gradient of all variables:

$$\frac{\partial u}{\partial y} = \frac{\partial v}{\partial y} = \frac{\partial T}{\partial y} = 0 \qquad (12)$$

On the wall, a non-slip condition is used:

$$u = v = 0 \qquad (13)$$

An insulation condition is assumed in all walls:

$$\frac{dT}{dx} = 0 \text{ on the vertical walls} \qquad (14)$$

$$\frac{dT}{dy} = 0 \text{ on the horizontal walls} \qquad (15)$$

RESULTS AND DISCUSSIONS

The commercial FLUENT 6.3.2 software package was used for solving the set of governing equations. The numerical method employed is based on the finite volume approach. Fluent provides flexibility in choosing discretization schemes for each governing equation. The discretized equations, along with the initial condition and boundary conditions, were solved using the segregated solution method. Using the segregated solver, the conservation of mass and momentum were solved sequentially and a pressure-correction equation was used to ensure the conservation of momentum and the conservation of mass (continuity equation).

A second-order upwind discretization scheme was used for the momentum equation. These schemes ensured, in general, satisfactory accuracy, stability and convergence. SIMPLE algorithm was used for pressure-velocity coupling. The discretized equations are solved implicitly in sequence, starting with the pressure equation followed by the momentum equations, by the pressure correction equation, and finally by the energy equations. The convergence criterion was set equal to 10^{-4} for all parameters. Before the numerical analysis, the grid-independency of the exchanger system was simply checked using a different number of grids. The system was finally divided into 9271 nodes corresponding to 8727 cells in consideration of grid-independency and calculating efficiency.

In order to validate the developed algorithm, the heat transfer in PCM storage with internal fins for a two-dimensional case is solved numerically and the results are compared with those obtained analytically [16]. Fig. 2 show the comparison between the evolutions of the solid–liquid interface during time obtained numerically and predicted analytically by [16]. A comparison shows that there is excellent correlation between the results. This underlines the good accuracy of the method proposed in this work.
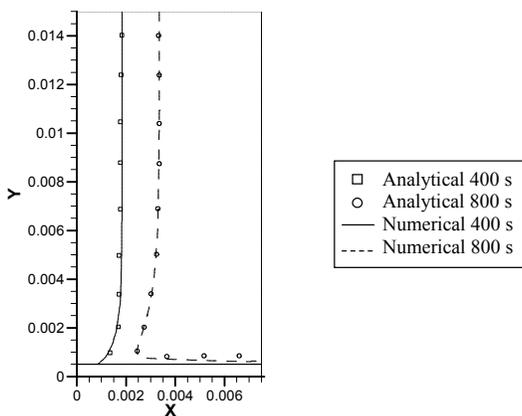
FIG.2. COMPARISON BETWEEN NUMERICAL AND ANALYTICAL POSITION OF SOLID–LIQUID INTERFACE.

Charging phase

We propose to study the effect the PCM thickness (quantity) contained in the exchanger. In the configuration (b)

the quantity of PCM was divided by two. Fig. 3 shows the effect of the PCM thickness on the liquid fraction evolution according to time during the storage phase. The blue color indicates the solid region ($f_\ell = 0$) and the red one indicates the liquid region ($f_\ell = 1$). During the storage phase, the initial temperature at all region is 293 K. At the entry, the temperature is fixed at 313 K with a mass flow of 0.01 kg/s. At $t = 5$ min, in the two configurations the fusion of the PCM starts in the vicinity of the entry which represents the thermal source of the exchanger. At $t = 30$ min, the fusion front reaches the bottom of the channel in the configurations (a) and (b). At $t = 40$ min, the fusion reaches 56% in the configuration (b) and 28% in the configuration (a). This percentage reaches 80% in the configuration (b) and 42% in the configuration (a) after 60 min. At $t = 80$ min, the fusion is complete in the configuration (b). In the configuration (a), the fusion reaches a percentage of 53%. At $t = 60$ min, the mass of the molten PCM reaches 12.77 and 12.24 kg in the configuration (a) and (b), respectively. Then, the increases of the PCM thickness (its quantity in the exchanger) do not influence considerably the storage speed (quantity of the PCM melted per second).
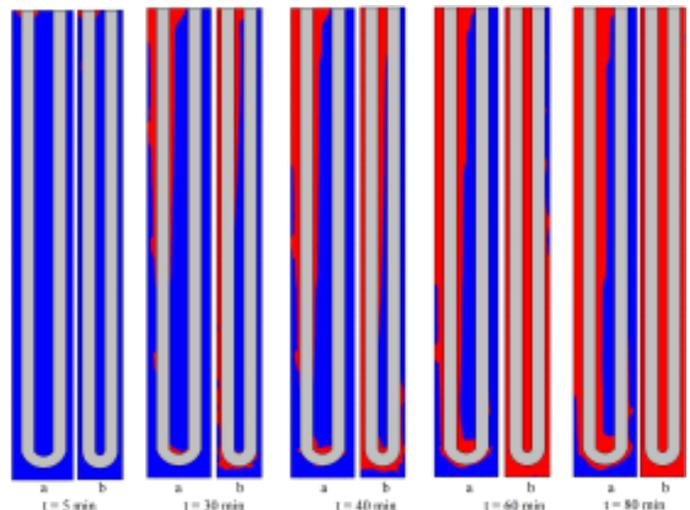
FIG. 3. EFFECT OF THE PCM THICKNESS ON THE LIQUID FRACTION EVOLUTION THE DURING THE STORAGE PHASE.

Fig. 4 shows the effect the PCM thickness on the temperature evolution vs. time during the storage phase. At $t = 5$ min, the two exchangers configurations are still out service since the outlet water temperatures are 293.15 K in the configuration (a) and 293,53 K in the configuration (b). Advancing in time, water warms up more and the PCM starts to store heat. After 30 min, the outlet water temperature increase in the configuration (b) and reaches 295.60 K, whereas the configuration (a) still out service and outlet temperature is 293.24 K. Since the PCM quantity used in the configuration (b) is less important than in the configuration (a), the PCM absorbs more heat from water in the configuration (a) and the outlet

temperature increases less rapidly. The same phenomenon is observed during time and at t = 80 min, the outlet water temperature reaches 296.81 K in the configuration (b) and 294.50 K in the configuration (a). The increase of the PCM quantity used influences considerably the outlet water temperature where the reduction reaches 2.31°C during 80 min of storage phase (temperature reduction speed is 1.73 °C/h). Finally, we can say that the configuration (b) is more dynamic when the configuration (a) stores more heat. Then, the configuration (b) is more adapted in zones with low solar radiation and the configuration (a) with high solar radiation.
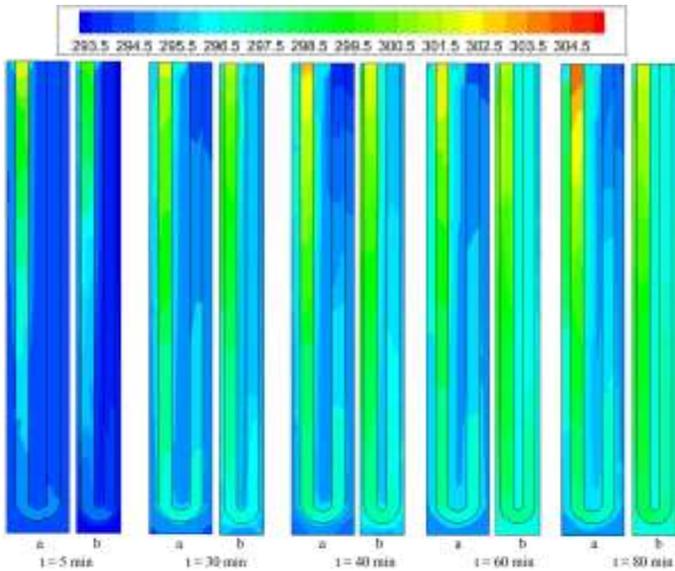
FIG. 4. EFFECT OF THE PCM THICKNESS ON THE TEMPERATURE [K] EVOLUTION DURING THE STORAGE PHASE.

The Fig. 5 shows the effect of the number of pass on the liquid fraction evolution vs. time during the storage phase. At t = 30 min, the PCM fusion percentage reaches 9.81% in the configuration (c) corresponding to 5.59 kg of PCM liquid mass. In the configuration (a), 21% of the PCM is molten offering 6.32 kg of PCM liquid mass. Thus, the fusion process is more accelerated in the configuration (a). At t = 103 min, the existing PCM between the two first pass is completely molten in the configuration (c). In the configuration (a), the PCM is molten between the two pass. The molten percentage is 38% and 65%, correspondent to PCM liquid mass of 21.9 and 19.5 kg in the configurations (c) and (a), respectively. One then records an acceleration of latent heat storage process in the configuration (c). At t = 285 min, the molten percentage is 66% and 100%, corresponding to PCM liquid mass of 37.8 and 28.25 kg in the configurations (c) and (a), respectively. There is an improvement of almost 9.5 kg in molten PCM corresponding to 1425 kJ of thermal energy stored in latent heat form, corresponding to an improvement of 300 kJ/h.
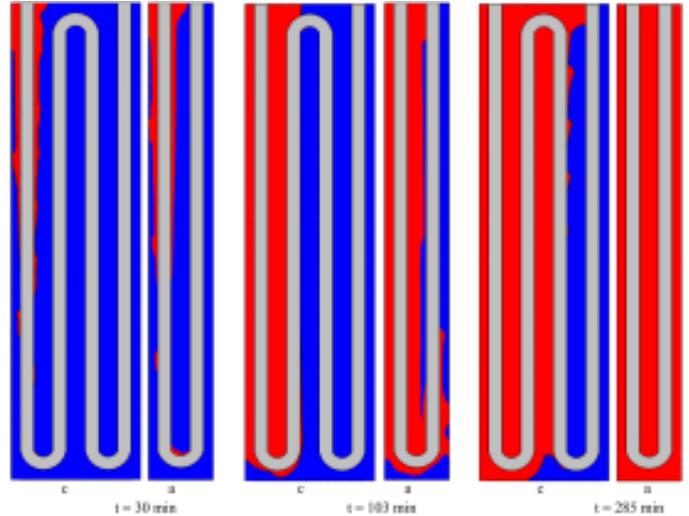
FIG. 5. EFFECT OF THE NUMBER OF PASS ON THE LIQUID FRACTION EVOLUTION DURING THE STORAGE PHASE.
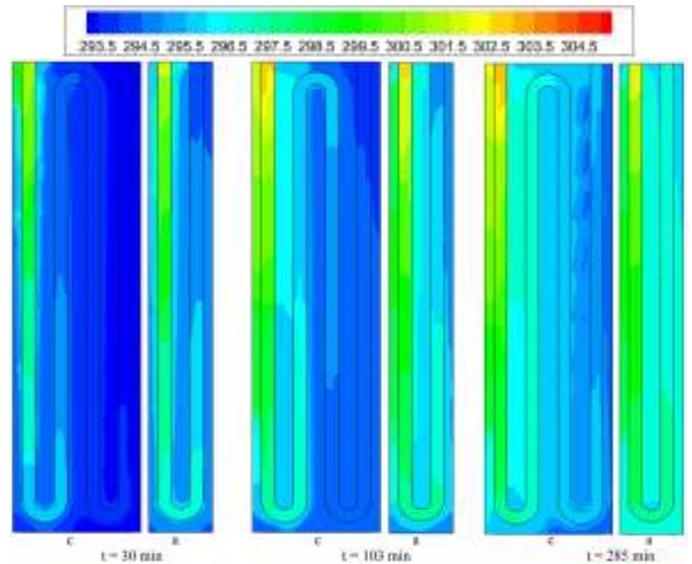
FIG. 6. EFFECT OF THE NUMBER OF PASS ON THE TEMPERATURE [K] EVOLUTION VS. TIME DURING THE STORAGE PHASE.

The Fig. 6 shows the effect of the number of pass on the temperature evolution vs. time during the storage phase. At t = 30 min, the temperature of water existing initially in channel starts to warm up and the two configurations of exchanger still out service since the outlet temperatures are 293.24 K in the configuration (a) and 293.34 K in the configuration (c). Advancing in time, water warms up more and the PCM starts to store heat. At t = 103 min, the outlet water temperature on the configuration (a) reaches 295.2 K and in the configuration (c) reaches 294.85 K. At t = 285 min, the outlet temperature reaches 297.07 K and 296.25 K in the configuration (a) and (c),

respectively. Then, we can say that the increase in the number of pass increases considerably the storage speed and thus the quantity of the PCM melted per second. This storage improvement does not influence considerably the outlet water temperature where the reduction reaches just 0.82°C during one storage period of 285 min; the speed of temperature reduction is 0.17 °C/h.
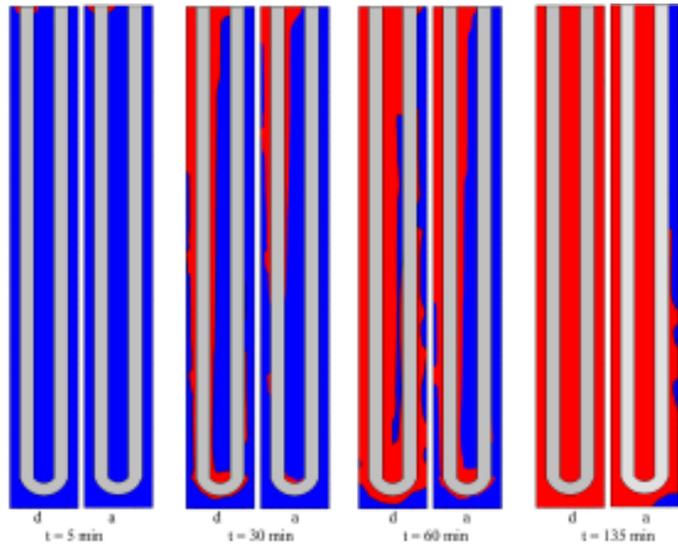
FIG. 7 . EFFECT OF WATER MASS FLOW ON THE LIQUID FRACTION EVOLUTION DURING THE STORAGE PHASE (a) 0.01 kg/s AND (d) 0.02 kg/s.

The Fig. 7 shows the effect of water mass flow on the liquid fraction evolution vs. time during the storage phase. At t = 5 min, the fusion of the PCM starts near the entry in the two configurations. At t = 30 min, the fusion of the PCM reaches 38% in the configuration (d) corresponding to a PCM liquid mass of 11.6 kg. In the configuration (a) 21% of the PCM is molten offering 6.32 kg of PCM liquid. Thus, the fusion process is accelerated in the configuration (d). Percentage of the molten PCM reaches 71% in the configuration (d) and 42% in the configuration (a) after 60 min. At t = 135 min, fusion process is complete in the configuration (d) but 79% of fusion is reached in the configuration (a). Then, there is an improvement of almost 3.4 kg in molten PCM corresponding to a 510 kJ of thermal energy stored in latent heat form (an improvement of 226.66 kJ/h).

Fig. 8 shows the effect of the water mass flow on the temperature evolution vs. time during the storage phase. At t = 5 min, the water temperature in the channel starts to warm up in the two configurations that still out service since the outlet water temperatures are 293.15 K and 293.24 K in the configuration (a) and (d), respectively. At t = 30 min, the outlet temperature increases in the configuration (d) and reaches 296.57 K, whereas the configuration (a) is still out service with an outlet temperature of 293.24 K. The same phenomenon is observed during the all storage period and at 135 min the

configuration (d) provides water at 298.07 K and the configuration (a) at 296.59 K. The improvement of heat storage influences the outlet water temperature where the reduction reached 1.48 °C during a storage period of 135 min; the temperature speed reduction is 0.65°C/h.
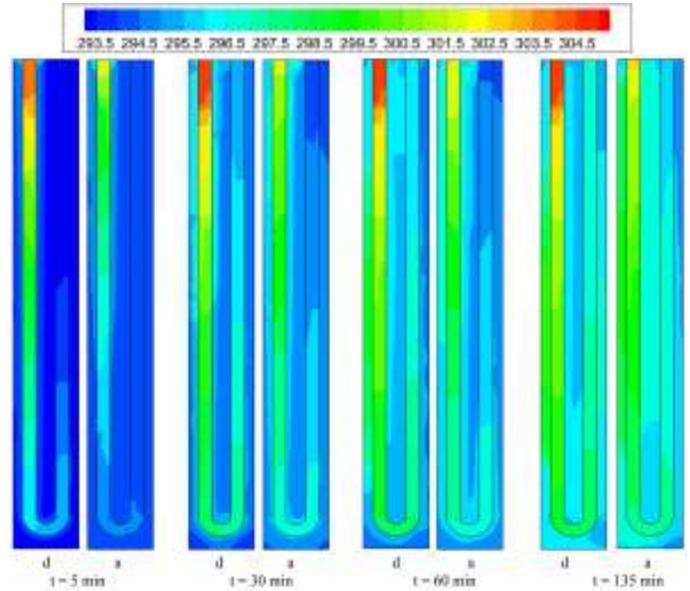
FIG. 8. EFFECT OF WATER MASS FLOW ON THE TEMPERATURE EVOLUTION VS. TIME DURING THE STORAGE PHASE (a) 0.01 kg/s AND (d) 0.02 kg/s.

Discharging phase:
The study of the discharging phase is started at the end of the charging (storage) phase.
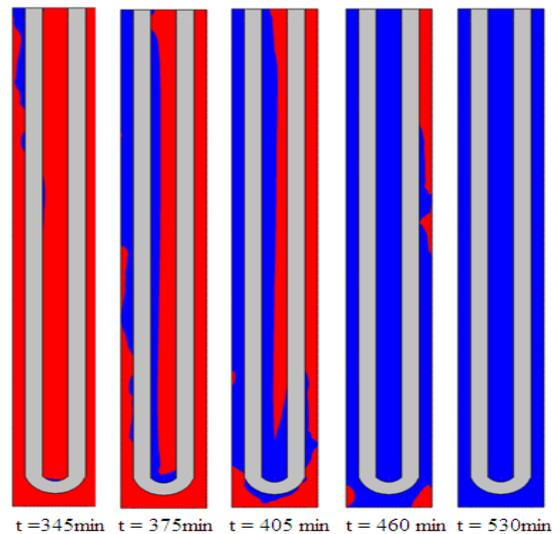
FIG. 9. EVOLUTION OF SOLIDIFICATION PROCESS VS. TIME DURING DISCHARGING PHASE.

The Fig. 9 shows the evolution liquid fraction vs. time during discharging phase. At t = 315 min, a fixed temperature of 285 K is imposed at the entry of the channel with a mass flow of 0.01 kg/s. At t = 345 min, a PCM solidification of 22.6% was reached corresponding to a mass of solid PCM of 5 kg. A solidification process continues to progress and reaches a percentage of 93.9% corresponding to 26.55 Kg of solid PCM after 460 min. At t = 530 min, a solidification process is complete.
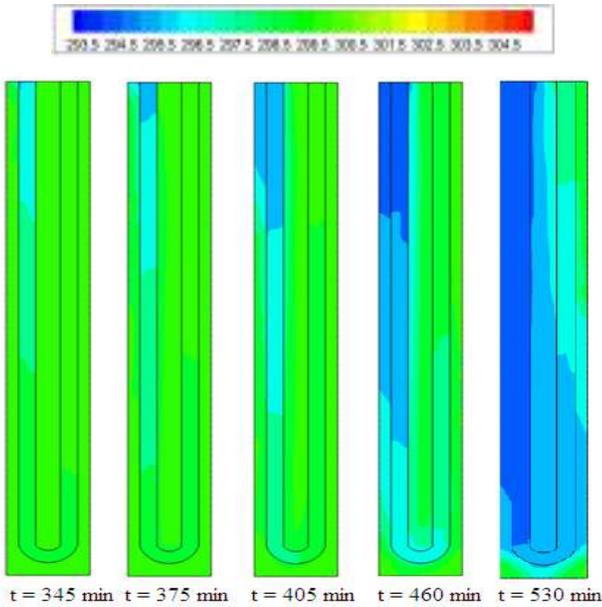
FIG. 10. EVOLUTION OF TEMPERATURE VS. TIME DURING THE DISCHARGING PHASE.
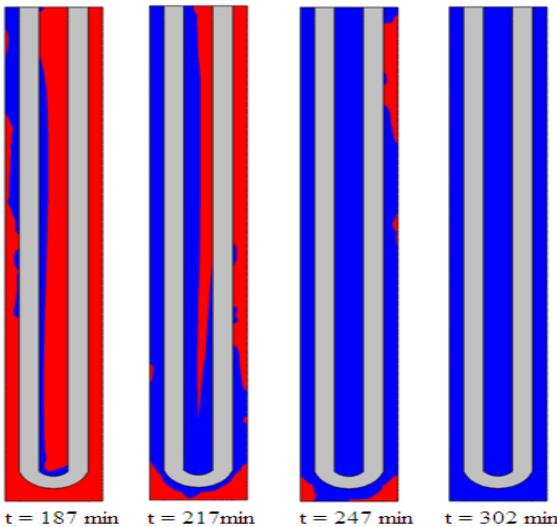
FIG. 11. EVOLUTION OF SOLIDIFICATION PROCESS VS. TIME DURING THE DISCHARGING PHASE.

Fig. 10 shows the temperature evolution vs. time during the discharging phase. At t = 345 min, the water temperature in channel starts to increases by absorbing heat from the PCM which undergoes a cooling, the outlet water temperature is 296.99 K. Advancing in time, water warms up more and the PCM continuous to lose it heat. At t = 375 min, the outlet water temperature reaches 296.74 K. At t = 530 min, the outlet water temperature is 293.17 K.

Fig. 11 shows the evolution of liquid fraction vs. time during the discharging phase. At t = 315 min, a fixed temperature of 285 K is imposed at the entry of the channel with a mass flow of 0.02 kg/s. At t = 187 min, one attends the solidification of 33.35% of the PCM corresponding to a solid mass in PCM of 8.22 kg. At t = 217 min, the solidified percentage reached is 69.86% corresponding to a solid mass of 19.2 kg. At t = 247 min, the percentage arrives at 86.04% with 24.06 kg of solid in PCM. At t = 302 min, a solidification is complete.
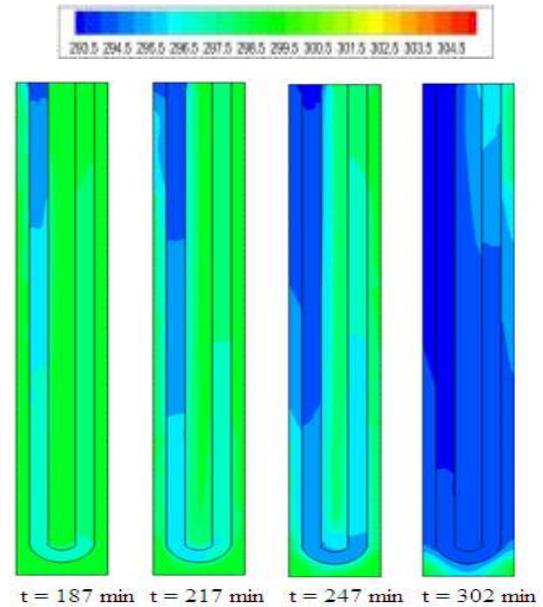
FIG. 12. EVOLUTION OF TEMPERATURE VS. TIME DURING THE DISCHARGING PHASE.

Fig. 12 shows the temperature evolution vs. time during the discharging phase. At t = 187 min, the water temperature begins to warm whereas the PCM starts to cool by yielding stored heat, the outlet water temperature arrives at 296.26 K. During time, water warms up more and the PCM continuous to lose heat and at t = 217 min the outlet temperature becomes 295.61 K. At t = 302 min the exchanger provides water at 290.69 K.

In the discharging phase, the speeds of solidification in the two configurations (a) and (d) are 0.131 kg/min and 0.171 kg/min, respectively. Then, there is an improvement of almost 2.4 kg/h in the PCM solidification corresponding to a thermal energy recuperation of 360 kJ/h for the configuration (d). It is

noticed that the speeds of the outlet temperature reduction in the two configurations (a) and (d) are 1.08°C/h and 2.76°C/h, respectively. Therefore, the increase in the water flow improves considerably the discharging process which influences the outlet water temperature. During charging and discharging phases the configuration (d) offers an acceleration in the process fusion-solidification of 4.4 kg/h correspondent to a thermal energy of 660 KJ/h.

CONCLUSION

The objective of present study is the latent heat thermal storage of a water heat exchanger using a phase change material PCM. Numerical simulation was carried out to investigate the solidification phenomenon development and temperature contours evolution at various components of the water exchanger. The problem was simulated and resolved using the commercial FLUENT computer code.

The governing equations, i.e. the conservation of mass, momentum and energy equations give us the tools necessary to deal mathematically with these applications. To simulate the phase change phenomenon the enthalpy-porosity method was adopted. The effects of the PCM thickness (mass quantity), the number of pass and the water mass flow on the thermal effectiveness of the exchanger were examined. The obtained results show clearly the influence as of these parameters on the thermal effectiveness of the exchanger.

Increasing the quantity of the PCM used influences considerably the outlet water temperature where the reduction can reaches 2.31°C during one period of 80 min, by doubling the PCM quantity. Reducing the quantity of the PCM used in the exchanger is more adapted in zones with low solar radiation.

Increasing the number of pass in the exchanger causes acceleration in the PCM melting process. This acceleration can reaches a formation of almost 9.5 kg of the liquid PCM corresponding to thermal energy storage of 1425 kJ, by doubling the number of pass. This improvement of heat storage does not influence considerably the outlet water temperature where the reduction reaches hardly 0.82°C during one period of 285min.

Increasing the water mass flow involves the acceleration of the melting process of PCM. Indeed, increasing the mass flow involves the increasing of the heat flow exchanged by forced convection. While passing from 0.01 kg/s to 0.02 kg/s we records an improvement of almost 3.4 kg in liquid PCM formed corresponding to a thermal energy stored of 510 kJ.

Increasing the water mass flow improves considerably the discharging process which influences the outlet water temperature. Speeds of the outlet temperature reduction are 1.08°C/h and 2.76°C/h for a mass flow of 0.01 kg/s and 0.02 kg/s, respectively. During two phases charging and discharging the model (d) offers acceleration in the process fusion-solidification of 4.4 kg/h corresponding to a thermal heat energy exchanged of 660 KJ/h.

REFERENCES

[1] N.A.M. Amin, F. Bruno, M. Belusko, Effectiveness–NTU correlation for low temperature PCM encapsulated in spheres, Applied Energy 93 (2012) 549–555.

[2] B. Basal, A. Unal, Numerical evaluation of a triple concentric-tube latent heat thermal energy storage, Solar Energy 92 (2013) 196–205

[3] S. Karthikeyan, G. Ravikumar Solomon, V. Kumaresan, R. Velraj, Parametric studies on packed bed storage unit filled with PCM encapsulated spherical containers for low temperature solar air heating applications, Energy Conversion and Management 78 (2014) 74–80

[4] A. Sharma, V.V. Tyagi, C.R. Chen, D. Buddhi, Review on thermal energy storage with phase change materials and applications, Renewable and Sustainable Energy Reviews 13 (2009) 318–345

[5] M. K. Rathod, J. Banerjee, Thermal stability of phase change materials used in latent heat energy storage systems: A review, Renewable and Sustainable Energy Reviews 18 (2013) 246–258

[6] N. Soares, J.J. Costa, A.R. Gaspar, P. Santos, Review of passive PCM latent heat thermal energy storage systems towards buildings' energy efficiency, Energy and Buildings 59 (2013) 82–103

[7] G. Selka, A. N. Korti, S. Abboudi, R. Saim, Numerical study of thermal behaviour of building walls containing a phase change material MECHANIKA. 2014 Volume 20(4), 367-375

[8] G. Selka, A. N. Korti, S. Abboudi, Dynamic thermal behavior of building using phase change materials for latent heat storage, Thermal Science, 2014 OnLine-First(00):134-134, DOI:10.2298/TSCI140311134S

[9] A. Castell, M. Belusko, F. Bruno, L.F. Cabeza, Maximisation of heat transfer in a coil in tank PCM cold storage system, Applied Energy 88 (2011) 4120-4127.

[10] A.A. Rabienataj Darzi, S.M. Moosania, F.L. Tanc, M. Farhadi, Numerical investigation of free-cooling system using plate type PCM storage, International Communications in Heat and Mass Transfer 48 (2013) 155–163.

[11] P. Omojaro, C. Breitkopf, Investigating and modeling of simultaneous charging and discharging of a PCM heat exchanger, Energy Procedia 48 (2014) 413 – 422.

[12] P. Charváta, L. Klimesa, M. Ostry, Numerical and experimental investigation of a PCM-based thermal storage unit for solar air systems, Energy and Buildings 68 (2014) 488–497.

[13] A. Hasan, S.J. McCormack, M.J. Huang, B. Norton, Characterization of phase change materials for thermal control of photovoltaics using Differential Scanning Calorimetry and Temperature History Method, Energy Conversion and Management 81 (2014) 322–329.

[14] A.D. Brent, V.R. Voller, K.J. Reid, Enthalpy-Porosity Technique for Modeling Convection-Diffusion Phase

Change: Application to the Melting of a Pure Metal, Numer. Heat Transfer, 13 (1988) 297-318.

[15] A.N. KORTI, A numerical simulation of convective flow in the solidification process, International Journal of Computational Methods, 7 4 (2010) 1–17.

[16] F. Talati, A.H. Mosaffa, M.A. Rosen, M. A., Analytical approximation for solidification processes in PCM storage with internal fins: imposed heat flux, Heat Mass Transfer 47 (2011) 369–376.